

Measurements from the brain

Simula summer school

26.6.2018

Tuomo Mäki-Marttunen

Measurements at different spatial scales

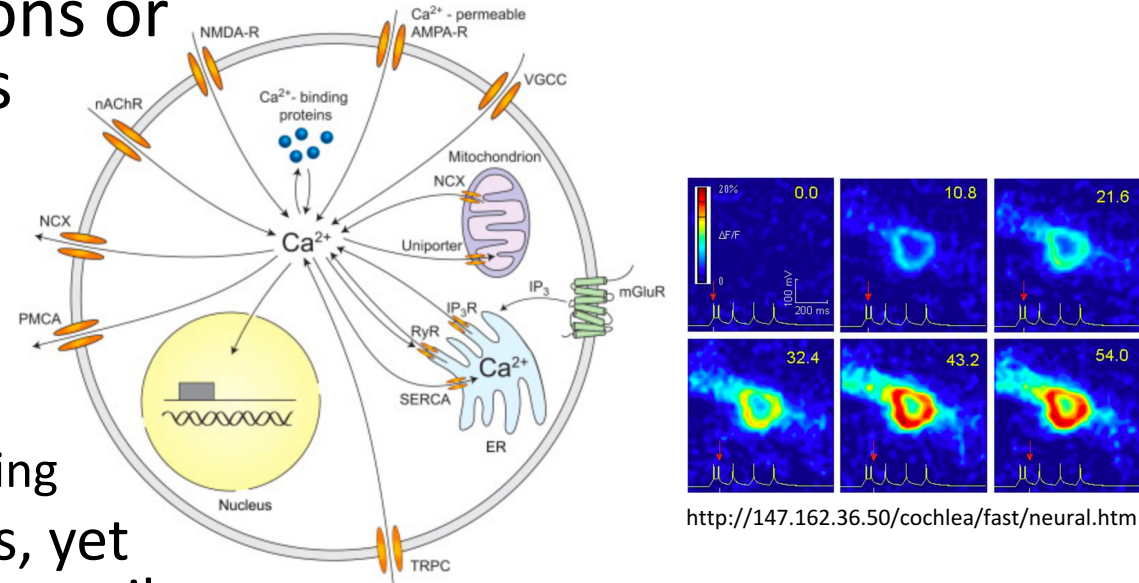
- *Ex vivo*/animal studies *in vivo*:
 - Standard electrophysiology
 - Ca^{2+} imaging
 - Voltage-sensitive dye (VSD) imaging
- Invasive animal/human measurements
 - Electrocorticography (ECoG)
- Noninvasive measurements
 - Electroencephalography (EEG)
 - Magnetoencephalography (MEG)
 - Magnetic resonance imaging (MRI)

Electrophysiological recordings of neurons

- Current clamp: Measure membrane currents
- Voltage clamp: Measure membrane potential
 - In both methods, the cell membrane is typically pierced by a sharp electrode
- Patch clamp
 - Patch pipette tightly sealed to the cell membrane
 - Many types of techniques: Cell-attached patch, whole cell patch, inside-out patch, outside-out patch, etc.

Ca^{2+} imaging of neurons

- Based on membrane-impermeant Ca^{2+} indicator molecules/proteins
- Neurons have a low intracellular Ca^{2+} concentration (50–100 nM)
 - May rise hundred-fold due to stimulation
- High-resolution imaging of single neurons or imaging of a whole network of neurons
- Problems:
 - Temporal resolution not as high as in electrophysiological recordings
 - Ca^{2+} binding required
 - -> Indicators alter the intracellular Ca^{2+} signaling
 - Heavily affected by supra-threshold inputs, yet difficult to differentiate between successive spikes

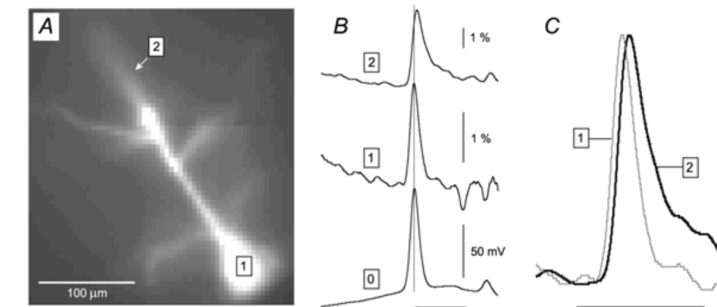


<http://147.162.36.50/cochlea/fast/neural.htm>

Grienberger, Christine, and Arthur Konnerth. "Imaging calcium in neurons." *Neuron* 73.5 (2012): 862-885.

VSD imaging of neurons

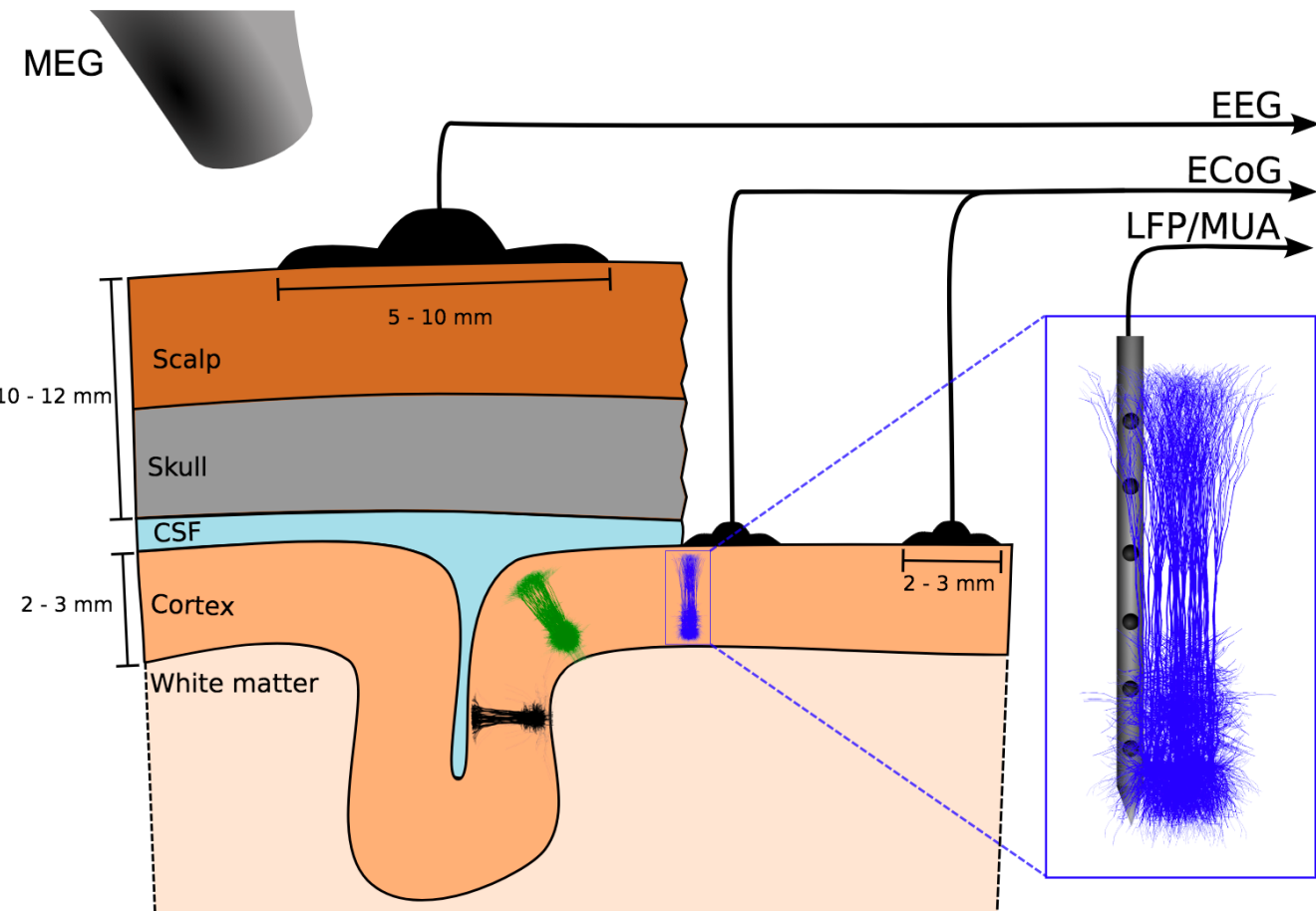
- Based on membrane-anchored voltage-indicating molecules
- Relatively high temporal resolution, typically limited by the speed of the microscope camera
- Problems:
 - Very sensitive to distance from the membrane
 - Limited number of VSD molecules at the plasma membrane -> extensive averaging needed
 - VSD molecules may anchor to internal membranes
 - Large numbers of VSD molecules at the membrane may alter the dynamical functions of the membrane



Antic, Srdjan D. "Action potentials in basal and oblique dendrites of rat neocortical pyramidal neurons." *The Journal of physiology* 550.1 (2003): 35-50.

ECoG, EEG, MEG

- Based on electrical dipole properties of the neuron that affect the local field potentials (LFPs) and the magnetic fields
 - Current flows into the neuron at certain locations and out at other locations
 - Single-cell contributions small, but synchronized activity of thousands or millions of neurons can be observed



Hagen, Espen, et al. "Multimodal modeling of neural network activity: computing LFP, ECoG, EEG and MEG signals with LFPy2. 0." *bioRxiv* (2018): 281717.

Forward modelling of the LFPs

- Poisson equation: $\nabla \cdot (\sigma_e(\mathbf{r}) \nabla \phi(\mathbf{r}, t)) = -C(\mathbf{r}, t)$
- Extracellular potential: $\phi(\mathbf{r}, t) = \frac{1}{4\pi\sigma_e} \frac{I(t)}{|\mathbf{r} - \mathbf{r}'|}$
- Point source approximation: $\phi(\mathbf{r}, t) = \frac{1}{4\pi\sigma_e} \sum_{j=1}^N \sum_{n=1}^{n_j^{\text{seg}}} \frac{I_{jn}^m(t)}{|\mathbf{r} - \mathbf{r}_{jn}|}$
- Line source approximation:
$$\begin{aligned} \phi(\mathbf{r}, t) &= \frac{1}{4\pi\sigma_e} \sum_{j=1}^N \sum_{n=1}^{n_j^{\text{seg}}} I_{jn}^m(t) \int \frac{1}{|\mathbf{r} - \mathbf{r}_{jn}|} d\mathbf{r}_{jn} \\ &= \frac{1}{4\pi\sigma_e} \sum_{j=1}^N \sum_{n=1}^{n_j^{\text{seg}}} \frac{I_{jn}^m(t)}{\Delta s_{jn}} \ln \left| \frac{\sqrt{h_{jn}^2 + r_{\perp jn}^2} - h_{jn}}{\sqrt{l_{jn}^2 + r_{\perp jn}^2} - l_{jn}} \right| \end{aligned}$$

- Assumed a constant conductivity σ_e
 - Not the case in EEG measurements

Hagen, Espen, et al. "Multimodal modeling of neural network activity: computing LFP, ECoG, EEG and MEG signals with LFPy2. 0." *bioRxiv* (2018): 281717.

Forward modelling of the EEGs

- When conductivity σ_e is not constant, alternative solutions for the Poisson equation

$$\nabla \cdot (\sigma_e(\mathbf{r}) \nabla \phi(\mathbf{r}, t)) = -C(\mathbf{r}, t)$$

are needed

- For forward modelling of the EEG signals, a simple head model can be used to calculate contribution of

Radial dipoles:

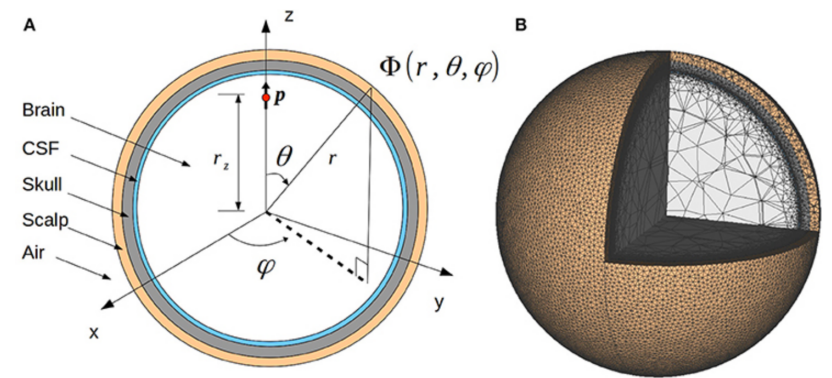
$$\Phi^1(r, \theta) = \frac{p}{4\pi\sigma_1 r_z^2} \sum_{n=1}^{\infty} \left[A_n^1 \left(\frac{r}{r_1} \right)^n + \left(\frac{r_z}{r} \right)^{n+1} \right] n P_n(\cos \theta) \quad r_z < r \leq r_1,$$

$$\Phi^s(r, \theta) = \frac{p}{4\pi\sigma_1 r_z^2} \sum_{n=1}^{\infty} \left[A_n^s \left(\frac{r}{r_s} \right)^n + B_n^s \left(\frac{r_s}{r} \right)^{n+1} \right] n P_n(\cos \theta) \quad r_{s-1} \leq r \leq r_s.$$

Tangential dipoles:

$$\Phi^1(r, \theta, \varphi) = \frac{-p}{4\pi\sigma_1 r_z^2} \sin \varphi \sum_{n=1}^{\infty} \left[A_n^1 \left(\frac{r}{r_1} \right)^n + \left(\frac{r_z}{r} \right)^{n+1} \right] P_n^1(\cos \theta) \quad r_z < r \leq r_1$$

$$\Phi^s(r, \theta, \varphi) = \frac{-p}{4\pi\sigma_1 r_z^2} \sin \varphi \sum_{n=1}^{\infty} \left[A_n^s \left(\frac{r}{r_s} \right)^n + B_n^s \left(\frac{r_s}{r} \right)^{n+1} \right] P_n^1(\cos \theta) \quad r_{s-1} \leq r \leq r_s,$$



Næss, Solveig, et al. "Corrected four-sphere head model for EEG signals." *Frontiers in human neuroscience* 11 (2017): 490.

Forward modelling of the MEG

- Magnetic field from dipole p can be calculated as

$$\mathbf{B}_p = \frac{\mu_0}{4\pi} \frac{\mathbf{p} \times \mathbf{R}}{R^3}$$

- Relation between magnetic fields measured by M and H :

$$\mathbf{B} = \mu_0 \mathbf{H} + \mathbf{M} = \mu \mathbf{H}$$

- In biological tissue, M is small

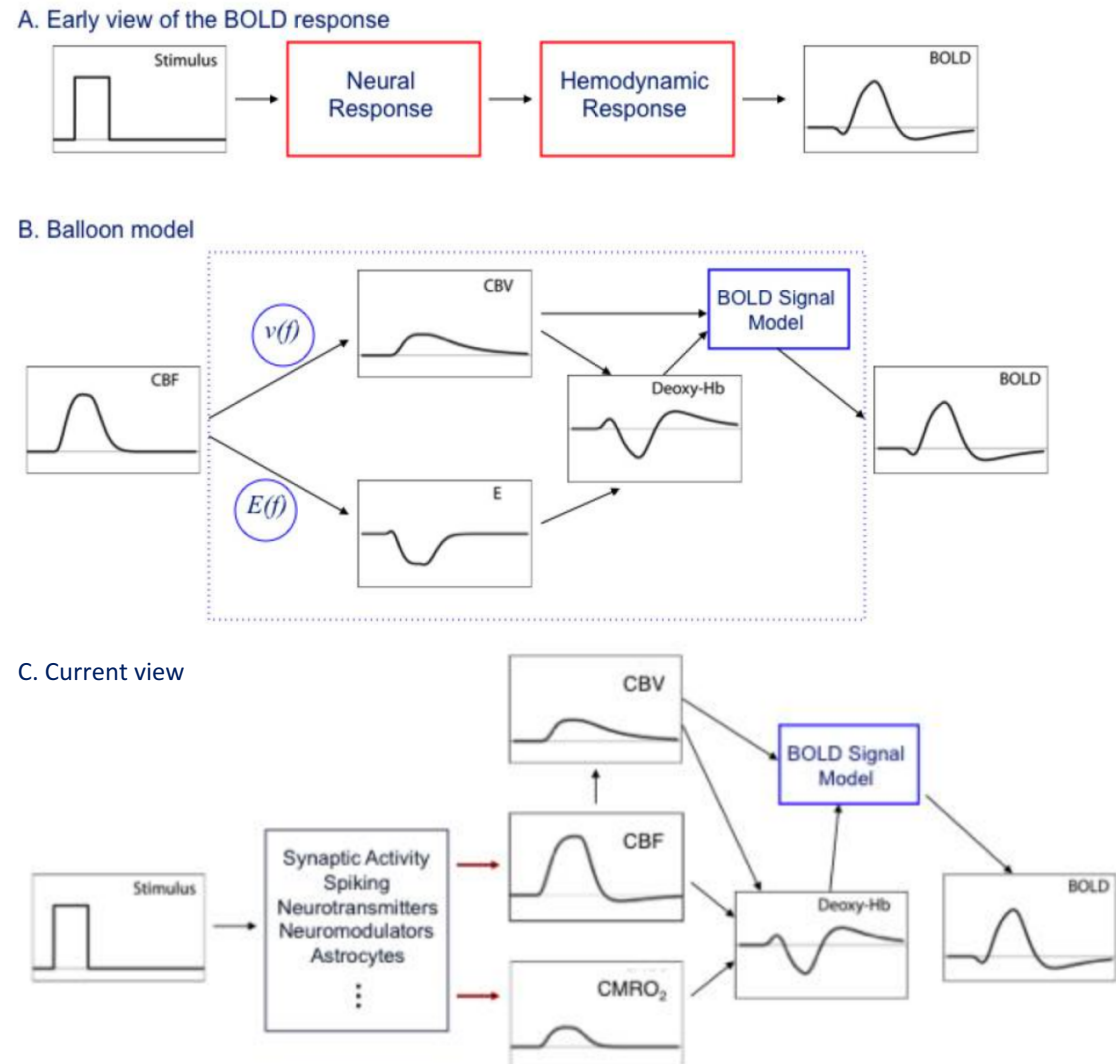
Magnetic resonance imaging

- Can be used to measure
 - Molecular diffusion -> diffusion tensor imaging (DTI)
 - Tissue composition → structural MRI
 - Changes in oxygen saturation-dependent magnetism of hemoglobin (blood-oxygen-level dependent (BOLD) signal) -> functional MRI (fMRI)
- High spatial resolution (millions of data points in 3D), low temporal resolution (typically ~ 0.5 Hz)



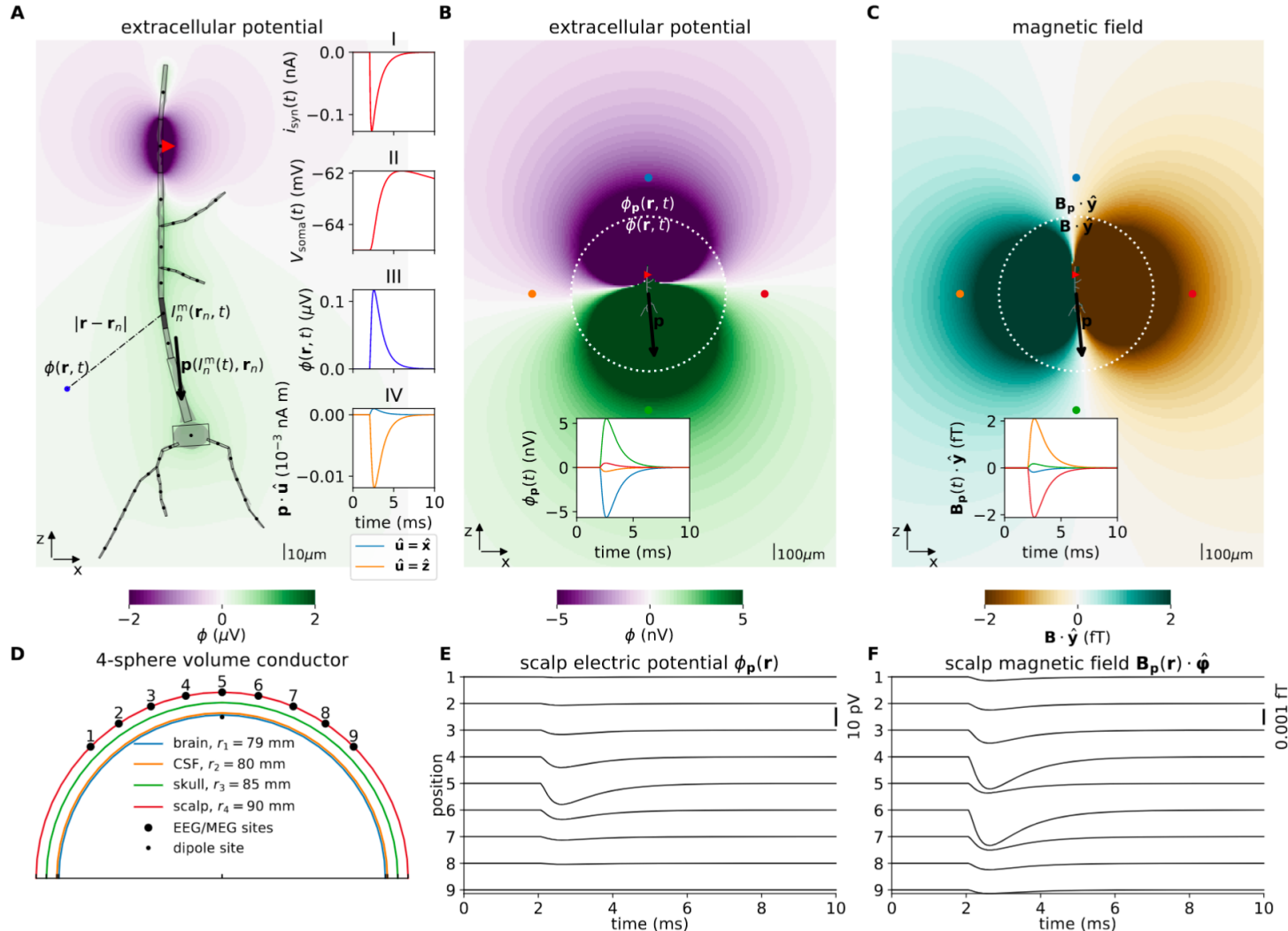
BOLD signal is widely adopted but difficult to model

- The BOLD signals stem from magnetic properties of the deoxyhemoglobin
- Neural activation decreases oxygen extraction fraction (E)
 - This depends on cerebral blood flow (CBF) and volume (CBV) and on the cerebral metabolic rate of oxygen (CMRO₂)



Buxton, Richard B. "Dynamic models of BOLD contrast." *Neuroimage* 62.2 (2012): 953-961.

LFPy toolbox: NEURON simulation with LFP recordings made easy



- <https://github.com/LFPy>

Hagen, Espen, et al. "Multimodal modeling of neural network activity: computing LFP, ECoG, EEG and MEG signals with LFPy2.0." *bioRxiv* (2018): 281717.